Electronic Supplementary Information (ESI) for

Self-assembly of transition-metal-oxide nanoparticle supraparticles with designed architectures and their enhanced lithium storage properties

Guannan Guo,[ab] Li Ji,[b] Xiudi Shen,[ab] Biwei Wang,[b] Hanwen Li,[b] Jianhua Hu,[a] Dong Yang*[a] and Angang Dong*[b]

[a]*State Key Laboratory of Molecular Engineering of Polymers and Department of Macromolecular Science, Fudan University, Shanghai 200433, China.*

[b]*Collaborative Innovation Center of Chemistry for Energy Materials, Shanghai Key Laboratory of Molecular Catalysis and Innovative Materials, and Department of Chemistry, Fudan University, Shanghai 200433, China.*

*To whom correspondence should be addressed: agdong@fudan.edu.cn (A.D.); yangdong@fudan.edu.cn (Y. D.).

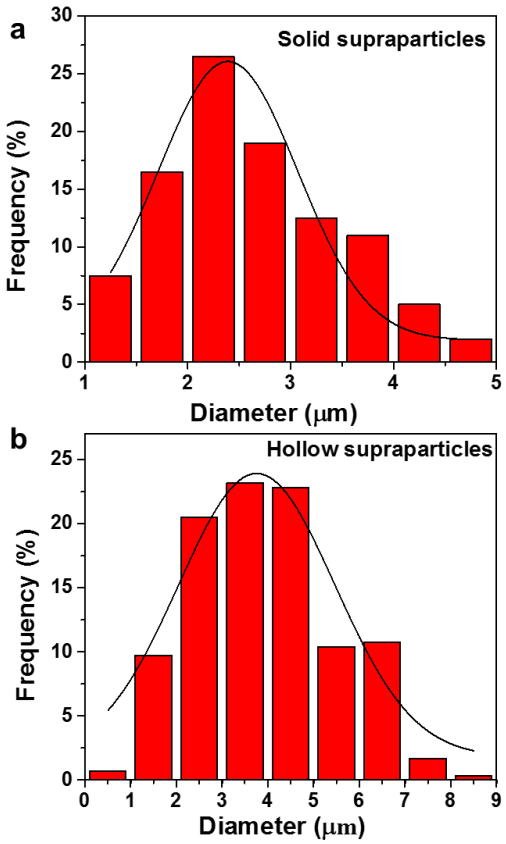

Figure S1. (a, b) Size distribution histograms of solid and hollow Fe_3O_4 NP supraparticles, respectively. The average diameter of solid and hollow Fe_3O_4 NP supraparticles was determined to be ~ 2.5 and 3.5 μm, respectively.

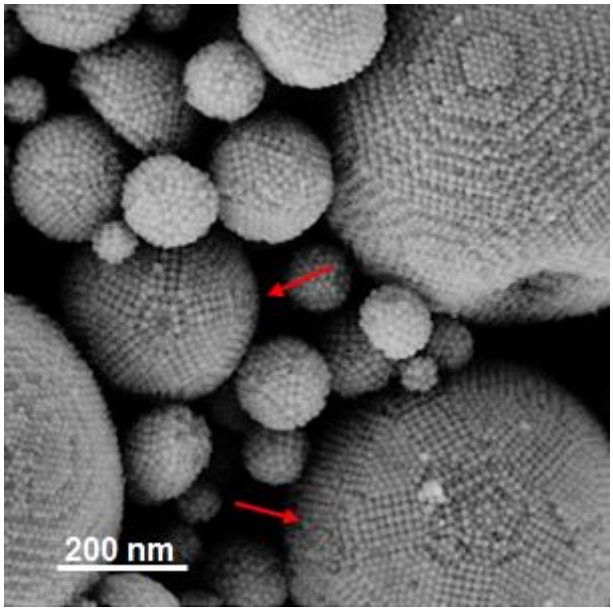

Figure S2. Representative HRSEM image of Fe_3O_4 NP supraparticles, showing the co-existence of icosahedral supraparticles (indicated by red arrows) with FCC supraparticles.

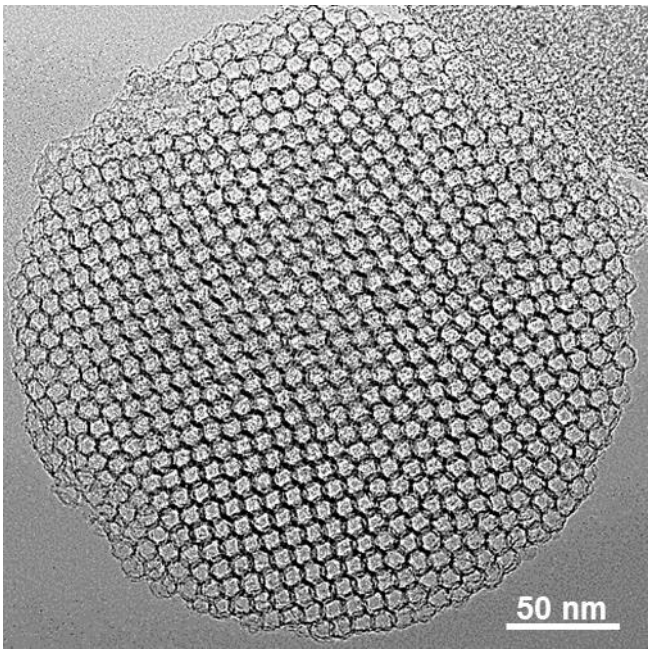

Figure S3. Typical TEM image of mesoporous carbon frameworks derived from the carbon-coated Fe_3O_4 NP supraparticles after acid etching. The 3D ordered carbon frameworks suggested the interconnection of carbon shells.

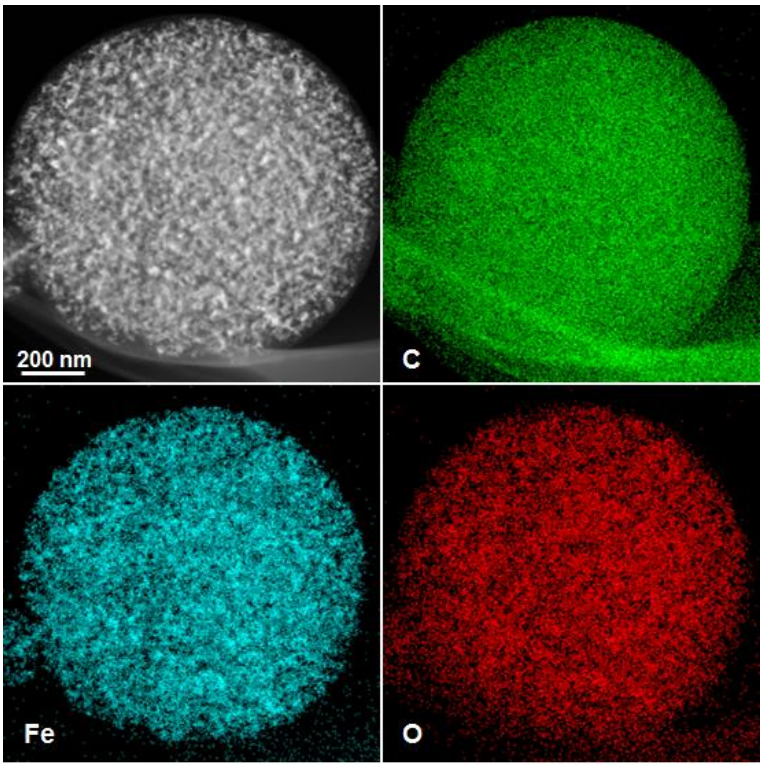

Figure S4. STEM image and the corresponding elemental mapping of a single Fe_3O_4 NP supraparticles after ligand carbonization. The homogeneous distribution of carbon suggested the formation of a 3D continuous carbon network after *in situ* ligand carbonization.

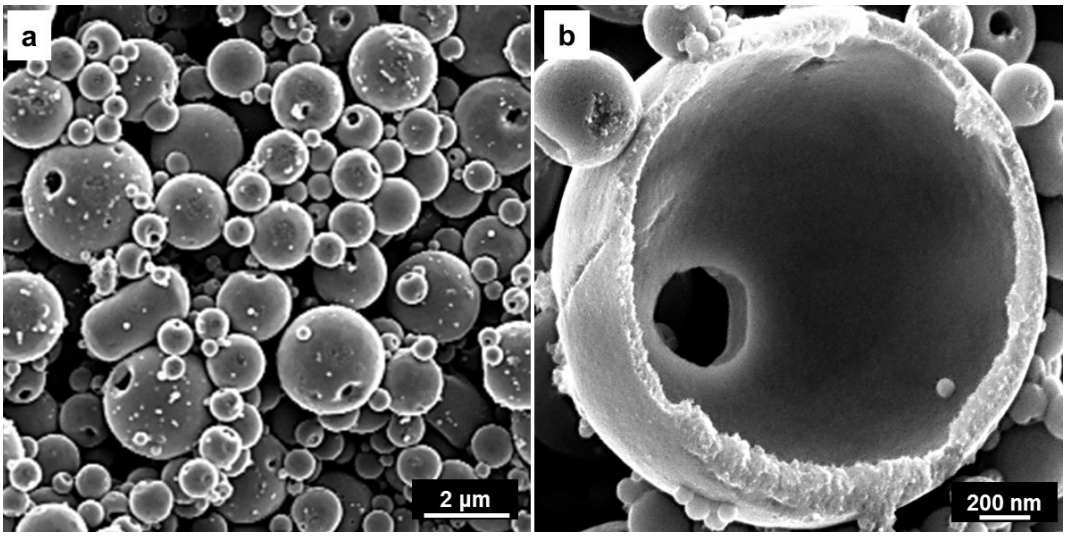

Figure S5. (a, b) SEM images of hollow supraparticles self-assembled from 6 nm $NiFe_2O_4$ NPs.

Table S1. Electrochemical performance of representative Fe_3O_4-based anodes reported previously.

Material	Current density (mA g^{-1})	Coulombic efficiency (1^{st} cycle)	Capacity (mAh g^{-1})	Ref.
Porous Fe_3O_4/VO_x/ graphene nanowires	100 2000		1164 808	S1
Fe_3O_4@Fe_3C-C yolk/shell nanospindles	500 2000	68.30%	1120 after 100 cycles 604.8	S2
CNT@Fe_3O_4@C coaxial nanocables	200 2000	65.50%	1290 after 80 cycles 690 after 200 cycles	S3
Graphene-wrapped Fe_3O_4 graphene nanoribbons	400		708 after 300 cycles	S4
Fe_3O_4/Fe nanocomposites	200 2000		390 after 50 cycles 260	S5
Hollow and yolk-shell Fe_3O_4 nanostructures	1000		585 after 100 cycles	S6
Fe_3O_4/carbon composite microspheres	2000 5000	72%	1022 for 150 cycles 733	S7
Fe_3O_4/SnO_2 coaxial nanofibers	100	74%	850 after 50 cycles	S8
Foam-like Fe_3O_4/C composite	200 5000		1008 after 400 cycles 580	S9
Novel Fe_3O_4-CNTs nanocomposite	92.8		850 after 100 cycles	S10
Carbon-coated Fe_3O_4 nanosheets	200 1000		1232 after 120 cycles 853	S11
Sandwich-structured Fe_3O_4@carbon	~ 100		860 after 100 cycles	S12
C@Fe_3O_4@C coaxial nanotubes	100	68%	1134 after 150 cycles	S13
Fe_3O_4 nanoparticles on graphene foam	924	68%	1200 after 500 cycles	S14
Fe_3O_4 nanoparticles on porous carbon	100 1000	61%	1462 after 100 cycles 676 after 500 cycles	S15
Hollow Fe_3O_4 NP supraparticles	1600	70.8%	1152 after 300 cycles	This work

References

S1. Q. An, F. Lv, Q. Liu, C. Han, K. Zhao, J. Sheng, Q. Wei, M. Yan and L. Mai, *Nano Lett.*, 2014, **14**, 6250-6256.

S2. J. Zhang, K. Wang, Q. Xu, Y. Zhou, F. Cheng and S. Guo, *ACS Nano*, 2015, **9**, 3369-3376.
S3. J. Cheng, B. Wang, C. Park, Y. Wu, H. Huang and F. Nie, *Chem - Eur. J.*, 2013, **19**, 9866-9874.
S4. L. Li, A. Kovalchuk, H. Fei, Z. Peng, Y. Li, N. D. Kim, C. Xiang, Y. Yang, G. Ruan and J. M. Tour, *Adv. Energy Mater.*, 2015, **5**, 1500171.
S5. M. Lübke, N. M. Makwana, R. Gruar, C. Tighe, D. Brett, P. Shearing, Z. Liu and J. A. Darr, *J. Power Sources*, 2015, **291**, 102-107.
S6. Z. Sun, K. Xie, Z. A. Li, I. Sinev, P. Ebbinghaus, A. Erbe, M. Farle, W. Schuhmann, M. Muhler and E. Ventosa, *Chem - Eur. J.*, 2014, **20**, 2022-2030.
S7. S. H. Choi, Y. N. Ko, K. Y. Jung and Y. C. Kang, *Chem - Eur. J.* 2014, **20**, 11078-11083.
S8. W. Xie, S. Li, S. Wang, S. Xue, Z. Liu, X. Jiang and D. He, *ACS Appl. Mater. Interfaces*, 2014, **6**, 20334-20339.
S9. F. Wu, R. Huang, D. Mu, B. Wu and S. Chen, *Appl. Mater. Interfaces*, 2014, **6**, 19254-19264.
S10. L. Yang, J. Hu, A. Dong and D. Yang, *Electrochim. Acta*, 2014, **144**, 235-242.
S11. G. Gao, S. Lu, B. Dong, Z. Zhang, Y. Zheng and S. Ding, *J. Mater. Chem. A*, 2015, **3**, 4716-4721.
S12. L. Zhao, M. Gao, W. Yue, Y. Jiang, Y. Wang, Y. Ren and F. Hu, *Appl. Mater. Interfaces*, 2015, **7**, 9709-9715.
S13. Q. Qu, J. Chen, X. Li, T. Gao, J. Shao and H. Zheng, *Nano Lett.*, 2015, **3**, 18289-18295.
S14. X. Hu, M. Ma, M. Zeng, Y. Sun, L. Chen, Y. Xue, T. Zhang, X. Ai, R. G. Mendes, M. H. Rümmeli and L. Fu, *Appl. Mater. Interfaces*, 2014, **6**, 22527-22533.
S15. L. Wang, L. Zhuo, C. Zhang and F. Zhao, *Chem - Eur. J.*, 2014, **20**, 4308-4315.